
The rule breaking $\text{Cr}_2(\text{CO})_{10}$. A 17 electron Cr system or a Cr=Cr double bond?

Se Li, Nancy A. Richardson, Yaoming Xie, R. Bruce King and Henry F. Schaefer III*

*Department of Chemistry and Center for Computational Quantum Chemistry,
University of Georgia, Athens, Georgia 30602, USA*

Received 7th November 2002, Accepted 9th January 2003

First published as an Advance Article on the web 28th April 2003

Density functional theory (DFT) has been used to investigate the conformations and thermochemistry on the singlet and triplet potential energy surfaces (PES) of $\text{Cr}_2(\text{CO})_{10}$. The global minimum energy structure for the lowest singlet state of C_{2h} symmetry is consistent with a model of two interacting $\text{Cr}(\text{CO})_5$ fragments in which one carbonyl in each fragment acts as an asymmetric four-electron donor bridging carbonyl, with chromium-chromium distances of 2.93 Å (B3LYP) or 2.83 Å (BP86). Avoiding a Cr...Cr bond by incorporating four-electron donor CO groups in this way allows each chromium atom in singlet $\text{Cr}_2(\text{CO})_{10}$ to attain the favored 18-electron configuration by using, in a simple picture of the bonding, only the six octahedral sp^3d^2 hybrids. The dissociation energy to two $\text{Cr}(\text{CO})_5$ fragments or to $\text{Cr}(\text{CO})_6 + \text{Cr}(\text{CO})_4$ fragments is predicted to be 10 kcal mol⁻¹. The lowest triplet state of $\text{Cr}_2(\text{CO})_{10}$ is predicted to lie ~10 kcal mol⁻¹ above the singlet global minimum. In the case of triplet $\text{Cr}_2(\text{CO})_{10}$ the lowest energy minima were found to be of C_2 and C_{2h} symmetry, with similar energies. The chromium-chromium distances in triplet $\text{Cr}_2(\text{CO})_{10}$ were found to be shorter than those in the corresponding singlet structures, namely 2.81 (B3LYP) or 2.68 Å (BP86) suggesting a $\sigma + 2(1/2) \pi$ Cr=Cr double bond similar to the O=O bond in O_2 or the Fe=Fe bond in the experimentally observed triplet state $(\text{Me}_5\text{C}_5)_2\text{Fe}_2(\mu\text{-CO})_3$.

1. Introduction

Recently our group has studied saturated homoleptic binuclear carbonyls of first row transition metals such as nickel,¹ iron,² and cobalt³ using carefully calibrated methods from density functional theory (DFT).⁴ The results are in reasonable agreement with available experimental values for geometries and thermodynamic quantities. These theoretical methods have been extended to unsaturated binuclear metal carbonyls. Optimized structures were found exhibiting the following features: (a) Metal–metal multiple bonds with the favored 18-electron rare gas metal electronic configuration such as formal M=M double bonds in $\text{Ni}_2(\text{CO})_6$ and $\text{Fe}_2(\text{CO})_8$, and formal M≡M triple bonds in $\text{Ni}_2(\text{CO})_5$, $\text{Co}_2(\text{CO})_6$, and $\text{Fe}_2(\text{CO})_7$; (b) Four-electron bridging carbonyl groups with the favored 18-electron metal electronic configuration such as in C_{2h} symmetry $\text{Fe}_2(\text{CO})_6$; (c) Metal electron configurations with fewer than 18 electrons, such as the 16-electron configurations for d^8 metal atoms found in unbridged $\text{Co}_2(\text{CO})_7$, analogous to the known⁵ $\text{CoRh}(\text{CO})_7$.

These results lead to further exploration of structures for as yet undetected unsaturated homoleptic binuclear carbonyls of the first row transition metals by DFT methods. This paper reports our $\text{Cr}_2(\text{CO})_{10}$ research. Simple electron counting⁶ indicates that if all ten CO groups are the

usual donors of two electrons each, then a Cr=Cr double bond is required to give each chromium atom the favored 18-electron configuration in $\text{Cr}_2(\text{CO})_{10}$.

Our previous results⁷ for the saturated homoleptic binuclear chromium carbonyl $\text{Cr}_2(\text{CO})_{11}$ showed this compound to have a flat potential energy surface and to be thermodynamically unstable with respect to dissociation^{8,9} to $\text{Cr}(\text{CO})_5$ and $\text{Cr}(\text{CO})_6$. This accounts for the experimental lack of $\text{Cr}_2(\text{CO})_{11}$ isolation. Substitution of the bridging CO in $\text{Cr}_2(\text{CO})_{11}$ with a hydride produces the stable and well-known $\text{HCr}_2(\text{CO})_{10}^-$, for which we also predicted the gas phase structure and compared it to two X-ray structures.^{10,11} Deprotonation of $\text{HCr}_2(\text{CO})_{10}^-$ results in the known $\text{Cr}_2(\text{CO})_{10}^{2-}$, which has also been structurally characterized.¹² Electrochemical experiments have examined the one-electron oxidation of $\text{Cr}_2(\text{CO})_{10}^{2-}$ to form $\text{Cr}_2(\text{CO})_{10}^-$ and the process of Cr–Cr bond cleavage.¹³ Two-electron oxidation of $\text{Cr}_2(\text{CO})_{10}^{2-}$ results in neutral $\text{Cr}_2(\text{CO})_{10}$. Transient (lifetime $\sim 10^{-3}$ s) $\text{Cr}_2(\text{CO})_{10}$ has been observed in photochemical studies in which $\text{Cr}(\text{CO})_4$ reacts with $\text{Cr}(\text{CO})_6$.¹⁴ These experimental results indicate that $\text{Cr}_2(\text{CO})_{10}$ may have greater stability than the unsaturated $\text{Cr}_2(\text{CO})_{11}$, and thus theoretical investigation of $\text{Cr}_2(\text{CO})_{10}$ has been undertaken to determine the nature of this molecule and reasons for its stability.

Since in some unsaturated binuclear metal compounds, the triplet state may lie lower in energy than the singlet, both electronic states are investigated for $\text{Cr}_2(\text{CO})_{10}$. The computed optimized structures for both the singlet and triplet states of the neutral $\text{Cr}_2(\text{CO})_{10}$ molecule are presented in Fig. 1 (singlet) and Fig. 2 (triplet). Analysis of the relationships between the geometries, harmonic vibrational frequencies and thermodynamic stabilities of the structures in each electronic state illustrate how the loss of two electrons perturbs the highly symmetric D_{4h} dianion $\text{Cr}_2(\text{CO})_{10}^{2-}$. These analyses also provide some insight into the nature of this unsaturated Cr–Cr bond as well as the difference in predictions between the B3LYP and BP86 functionals.

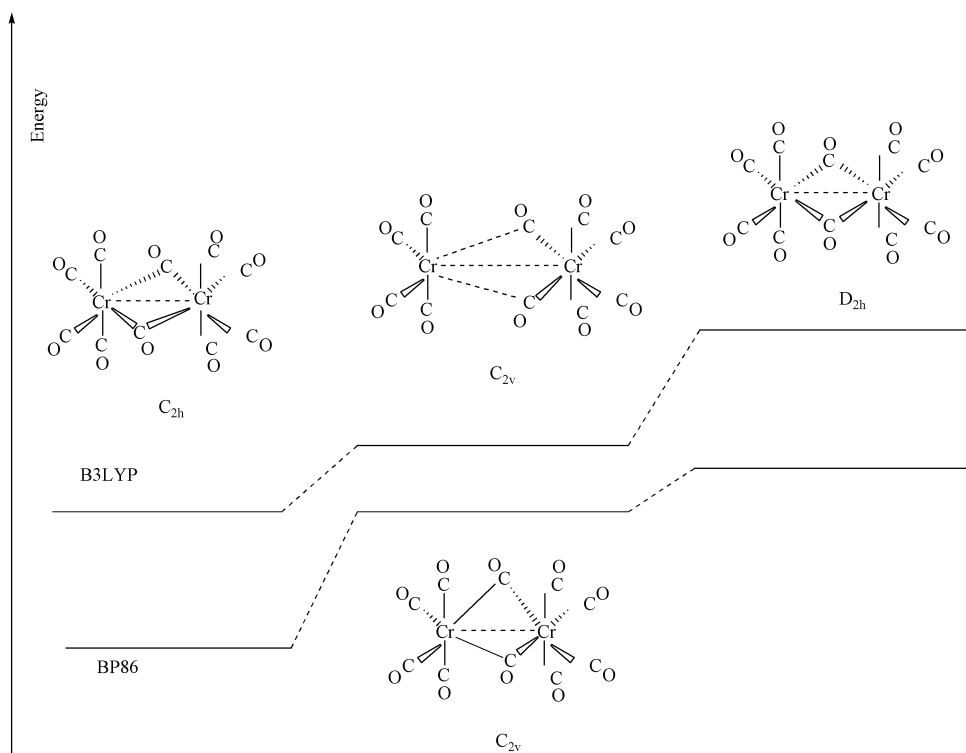


Fig. 1 Three singlet $\text{Cr}_2(\text{CO})_{10}$ structures predicted with the B3LYP and BP86 functionals. The energetic relationship of the structures is $E(C_{2h}) < E(C_{2v}) < E(D_{2h})$. Significant geometric differences exist between the B3LYP and BP86 methods for the C_{2v} structure.

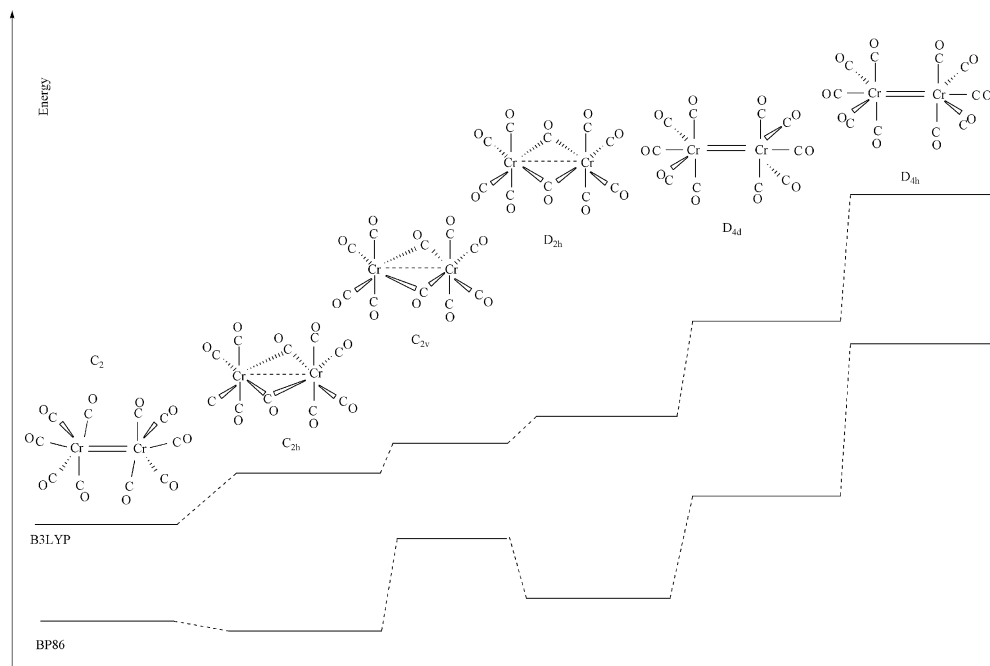


Fig. 2 Six triplet $\text{Cr}_2(\text{CO})_{10}$ structures predicted with the B3LYP and BP86 functionals. The energetic relationship of the structures is $E(\text{C}_2) < E(\text{C}_{2\text{h}}) < E(\text{C}_{2\text{v}}) < E(\text{D}_{2\text{h}}) < E(\text{D}_{4\text{d}}) < E(\text{D}_{4\text{h}})$ for the B3LYP functional, while it is $E(\text{C}_{2\text{h}}) < E(\text{C}_2) < E(\text{D}_{2\text{h}}) < E(\text{C}_{2\text{v}}) < E(\text{D}_{4\text{d}}) < E(\text{D}_{4\text{h}})$ for BP86.

2. Theoretical methods

Our basis set for C and O begins with Dunning's standard double- ζ contraction¹⁵ of Huzinaga's primitive sets¹⁶ and is designated (9s5p/4s2p). The double- ζ plus polarization (DZP) basis set used here adds one set of pure spherical harmonic d functions with orbital exponents $\alpha_{\text{d}}(\text{C}) = 0.75$ and $\alpha_{\text{d}}(\text{O}) = 0.85$ to the DZ basis set. For Cr, our loosely contracted DZP basis set, the Wachters primitive set,¹⁷ is used, but augmented by two sets of p functions and one set of d functions, contracted following Hood, Pitzer and Schaefer¹⁸ and designated (14s11p6d/10s8p3d). For $\text{Cr}_2(\text{CO})_{10}$, there are 398 contracted Gaussian functions in the present flexible DZP basis set.

Electron correlation effects were included employing DFT methods, which are acknowledged to be a practical and effective computational tool, especially for organometallic compounds.¹⁹ Among density functional procedures, the most reliable approximation is often thought to be the hybrid Hartree-Fock (HF)/DFT method, B3LYP, which uses the combination of the three-parameter Becke exchange functional with the Lee-Yang-Parr correlation functional.^{20,21} However, another DFT method, which combines Becke's 1988 exchange functional²² with Perdew's 1986 nonlocal correlation functional method (BP86),²³ has proven effective²⁴ and is also used in this research.

We fully optimized the geometries of all structures with the DZP B3LYP and DZP BP86 methods. At the same levels we also computed the vibrational frequencies by analytically evaluating the second derivatives of the energy with respect to the nuclear coordinates. The corresponding infrared intensities are evaluated analytically as well. All of the computations were carried out with the Gaussian 94 program,²⁵ exercising the fine grid (75 302) option for evaluating integrals numerically, and the tight ($10^{-8} E_{\text{h}}$) designation is the default for the self-consistent field (SCF) convergence. Cases for which finer integration grids were used are addressed below.

In the search for minima using all currently implemented DFT methods, low magnitude imaginary vibrational frequencies are suspect because of significant limitations in the numerical

integration procedures used. Thus, for an imaginary vibrational frequency with a magnitude less than 100 cm^{-1} , there is an energy minimum identical to or very close to the structure of the stationary point in question. Therefore, we generally do not follow such low imaginary vibrational frequencies. However, we reevaluated the D_{4h} structure of $\text{Cr}_2(\text{CO})_{10}$ with finer integration grids, but the small imaginary vibrational frequencies persisted. For low harmonic vibrational frequencies, the DFT methodology requires further development to yield rock solid predictions. However, continued efforts to discover and document patterns within systems which display these discrepancies will provide both direction in the development of DFT and insight into “unusual” bonding situations.

3. Results

3.1 The reliability of DFT for chromium carbonyls

Our previous work has shown that geometries and vibrational frequencies predicted using B3LYP and BP86 DFT functionals were in reasonable agreement ($\sim 0.02\text{ \AA}$ for bond distances) with experimental and higher level theoretical results for $\text{Cr}(\text{CO})_6$, $\text{Cr}(\text{CO})_5$, $[\text{Cr}(\text{CO})_5\text{H}]^-$, and $[\text{Cr}(\text{CO})_4\text{H}]^-$. In that work similar agreement was also found for $[(\mu\text{-H})\text{Cr}_2(\text{CO})_{10}]^-$, for which an experimental geometry is known. The prediction for the bridged species is similar to that for the solid crystal owing to the Cr–H interaction and the stabilizing nature of the bridging species. This is in contrast to the $[\text{Cr}_2(\text{CO})_{10}]^{2-}$ dianion which is predicted to have a somewhat longer Cr–Cr distance, (3.30 \AA , both functionals) than the experimental distances (2.98–3.00 \AA) for Cr–Cr in $[\text{Cr}_2(\text{CO})_{10}]^{2-}$ crystals^{26,27}. The difference between the isolated gas phase species, in which some bond lengthening is possible, and the constrained environment of the solid crystal may account for this difference in the dianion geometry. With only the dianion differing significantly from experimentally determined geometry (explainable by the effects of excess charge) these results would seem to indicate at least a qualitative reliability of DFT for these molecules.

3.2 Singlet $\text{Cr}_2(\text{CO})_{10}$

The fully optimized structures for the singlet electronic state of $\text{Cr}_2(\text{CO})_{10}$ (sketches in Fig. 1) are displayed in Figs. 3, 4, and 5. The relative energies of the structures and corresponding imaginary harmonic vibrational frequencies are listed in Table 1.

Fig. 3 shows the dibridged C_{2h} structure having all real harmonic vibrational frequencies; the electronic state is 1A_g . This structure is a genuine minimum with both the B3LYP and BP86 functionals and has the lowest energy among all nine neutral $\text{Cr}_2(\text{CO})_{10}$ structures examined here. In addition, the energy of the C_{2h} conformer is lower than that of two $\text{Cr}(\text{CO})_5$ fragments by 8.6

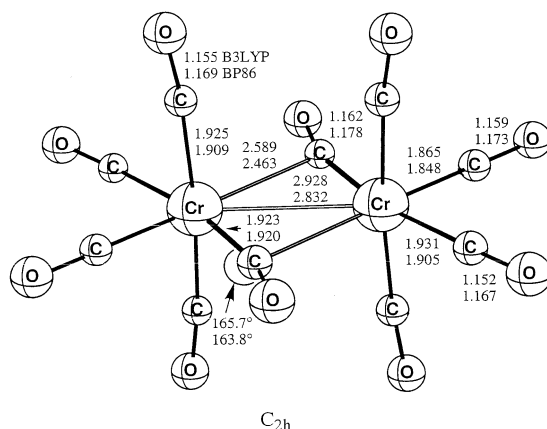
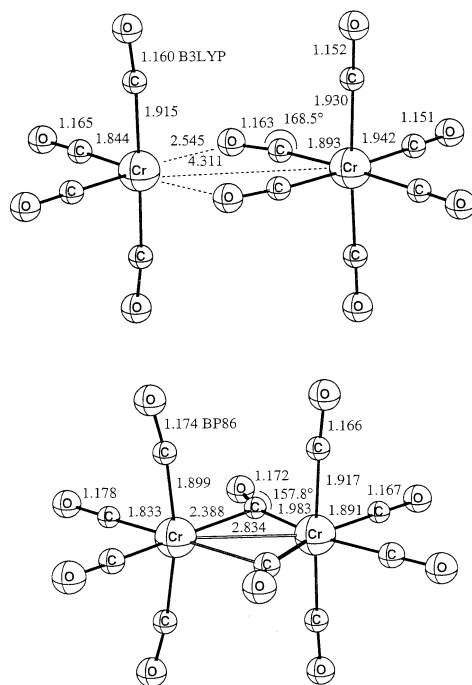


Fig. 3 The asymmetrically bridging C_{2h} global minimum energy structure for singlet $\text{Cr}_2(\text{CO})_{10}$ (all real harmonic vibrational frequencies) from the B3LYP and BP86 methods. Distances are reported in \AA .

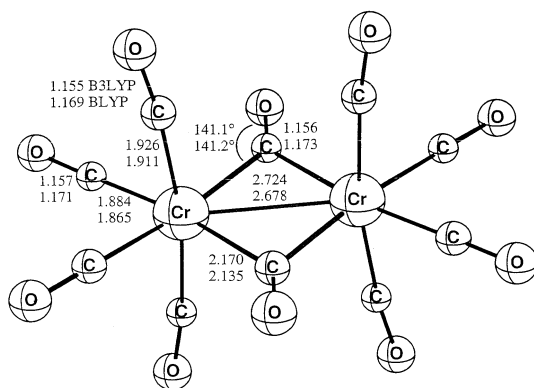


C_{2v}

Fig. 4 The second lowest energy singlet structure for $\text{Cr}_2(\text{CO})_{10}$, with C_{2v} symmetry, all real harmonic vibrational frequencies (B3LYP) and one large imaginary harmonic vibrational frequency (BP86). Distances are reported in Å.

(B3LYP) or $16.6 \text{ kcal mol}^{-1}$ (BP86), respectively. For fragmentation to $\text{Cr}(\text{CO})_6$ and $\text{Cr}(\text{CO})_4$ the energy differences are $7.9 \text{ kcal mol}^{-1}$ (B3LYP) and $15.1 \text{ kcal mol}^{-1}$ (BP86).

The relatively long Cr–Cr distance (B3LYP, 2.928 Å ; BP86, 2.832 Å) in the $\text{Cr}_2(\text{CO})_{10}$ structure of C_{2h} symmetry suggests that the $\text{Cr} \cdots \text{Cr}$ interaction takes place primarily through the π bonds of the bridging CO groups rather than through multiple bonding between the two chromium atoms.



D_{2h}

Fig. 5 The symmetrically dibridged singlet $\text{Cr}_2(\text{CO})_{10}$ structure with D_{2h} symmetry and one large imaginary harmonic vibrational frequency for both B3LYP and BP86. Distances are reported in Å.

Table 1 Relative energies of singlet Cr₂(CO)₁₀ and related structures

Species	Symmetry	State	Figure	Imaginary harmonic vibrational frequencies		Total energy/ <i>E_h</i>		Relative energy/kcal mol ⁻¹	
				B3LYP	BP86	B3LYP	BP86	B3LYP	BP86
Cr ₂ (CO) ₁₀	C _{2h} C _{2v}	¹ A _g ¹ A ₁	3	(none)	(none)	-3222.64440	-3223.06806	0.0	0.0
				348i(b ₂), 50i(a ₂), 40i(b ₁)	4a, 4b	-3222.64178	-3223.05547	1.6	7.9
2Cr(CO) ₅ Cr(CO) ₄ + Cr(CO) ₆	D _{2h}	¹ A _g	5	404i(b _{2g}), 153i(b _{3u}), 41i(b _{2u})	438i(b _{2g}), 78i(b _{3u}), 73i(b _{3g}), 70i(b _{2u})	-3222.62970	-3223.05462	9.2	8.4
				(none) (none)	(none) (none)	-3222.63069	-3223.04167	8.6	16.6
	C _{2v} , O _h	¹ A ₁ , ¹ A _g				-3222.63176	-3223.04393	7.9	15.1

The Cr–C distances of the four symmetry equivalent perpendicular terminal carbonyls are 1.925 Å (B3LYP) or 1.909 Å (BP86). The four unique Cr–C distances in the C–Cr–Cr–C plane are 1.923 Å for the shorter bridging Cr–C and 1.931 Å for the terminal Cr–C opposite to the shorter bridging Cr–C. Similarly, the distances are 2.589 Å for the longer bridging Cr–C and 1.865 Å for the terminal Cr–C opposite to the longer bridging Cr–C with the B3LYP method. With the BP86 functional the respective distances are 1.920 Å, 1.905 Å, 2.463 Å and 1.848 Å. The first two Cr–C distances in Cr₂(CO)₁₀ are very close to the analogous computed Cr–C distances in Cr(CO)₅ (1.923 Å B3LYP and 1.905 Å BP86), specifically the ¹A_g state of C₄ symmetry.⁷ However, the Cr–C distances for the remaining bridging carbonyls are much longer. The increased distance reflects the significantly weaker interaction in the bridging Cr–C compared to the terminal Cr–C distance computed for the Cr(CO)₅ fragment. The corresponding C–O distances are as follows: 1.155 Å, 1.159 Å, 1.162 Å and 1.152 Å with B3LYP and 1.169 Å, 1.173 Å, 1.178 Å and 1.167 Å with BP86, which are again nearly the same as the computed C–O distances in Cr(CO)₅ (1.162 Å with B3LYP and 1.171 with BP86). These distances also compare favorably with the experimentally known values in Cr(CO)₆ of 1.916 ± 0.002 Å (*r*_{Cr–C}) and 1.140 ± 0.003 Å (*r*_{C–O}).²⁸

Finally, consideration of the Cr–C–O angles for the shorter bridging carbonyl shows significant deviation from linearity at 165.7° (B3LYP) and 164.8° (BP86). This deviation is in accord with the proposed π-bonding from the C–O bond of this carbonyl to a chromium atom. The other four Cr–C–O angles do remain close to 180°. The C–Cr–C angles are also computed to be close to 90°, as shown in Fig. 3. Thus it is logical to conclude that the lowest energy structure for Cr₂(CO)₁₀ is an 18-electron species, in which the longer bridging carbonyls contribute two π electrons to complete the 18 electron configuration for each chromium atom.

Imposing C_{2v} symmetry forces the bridging carbonyls to produce the C_{2v} structure with an ¹A₁ electronic wavefunction. The two structures thus produced are shown in Fig. 4a (B3LYP) and 4b (BP86). With the B3LYP method this structure has no imaginary harmonic vibrational frequencies and is only 1.6 kcal mol⁻¹ higher than the C_{2h} structure. However, with the BP86 method this structure has one significantly large imaginary harmonic vibrational frequency of b₂ symmetry at 348i cm⁻¹ and two small imaginary vibrational frequencies at 50i (a₂) and 40i cm⁻¹ (b₁). The larger BP86 imaginary vibrational frequency corresponds to a return to the lower energy C_{2h} structure that lies 7.9 kcal mol⁻¹ lower. As discussed above, we only consider imaginary vibrational frequencies with magnitudes over 100 cm⁻¹ to be indisputable. This is another example showing that the B3LYP and BP86 are sometimes inconsistent in predicting the number of the imaginary frequencies for these metal dimers. In either case we conclude that the C_{2v} structure is not a genuine minimum but rather a higher order stationary point on the energy surface for BP86.

The geometric differences between the B3LYP and BP86 C_{2v} structures for singlet Cr₂(CO)₁₀ (Fig. 4) are also striking. Unexpectedly, the chromium-chromium distance is a very long 4.311 Å with the B3LYP functional. It appears that a loosely associated complex of Cr(CO)₄ and Cr(CO)₆ forms with a bridging Cr···O distance of 2.545 Å (B3LYP), implying that the two fragments have a very weak connection. However, with BP86 the Cr–Cr bond distance is 2.834 Å, which is essentially the same as the Cr–Cr bond distance in C_{2h} symmetry (2.832 Å, BP86). This C_{2v} structure behaves similarly to other binary homoleptic transition metal carbonyls where the B3LYP and BP86 methods sometimes lead to widely different structural predictions^{3,5} and so direct comparison cannot be made. However, in previous work the BP86 functional performed better for the prediction of the [(μ-H)Cr₂(CO)₁₀]⁻ structure, and similar confidence may be warranted here since the HF component without electron correlation can lead to the errors in B3LYP.

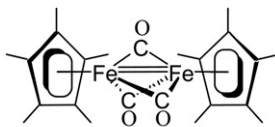
Imposition of further symmetry constraints produces the dibridged D_{2h} structure, the last of the singlet structures considered (Fig. 5). Both the B3LYP and BP86 functionals yield several imaginary vibrational frequencies above 100 cm⁻¹ for this structure, including the b_{2g} frequency at 404i cm⁻¹ (B3LYP) or 438i cm⁻¹ (BP86) and the b_{3u} frequency at 153i cm⁻¹ (B3LYP). These normal modes correspond to motions that reduce the symmetry to the lower energy C_{2v} and C_{2h} structures. Also, the D_{2h} structure is higher by 9.2 kcal mol⁻¹ (B3LYP) or 8.4 kcal mol⁻¹ (BP86) than the C_{2h} global minimum. Clearly, this symmetric dibridged Cr₂(CO)₁₀ structure is not a minimum. However, the predicted chromium–chromium distance for this structure is the shortest among the three singlet structures, namely 2.724 Å (B3LYP) or 2.678 Å (BP86) but obviously still in the range of a single bond. The dibridging Cr–C distance is 2.170 Å (B3LYP) or 2.135 Å (BP86) which is longer than the Cr–C distance in the Cr(CO)₅ fragment (1.923 Å B3LYP and 1.905 Å

BP86) and also longer than the experimental $\text{Cr}(\text{CO})_5$ distance of 1.916 Å. Thus we conclude that there is a Cr–Cr single bond in this structure.

3.3 Triplet $\text{Cr}_2(\text{CO})_{10}$

For singlet $\text{Cr}_2(\text{CO})_{10}$, stationary points were found for three symmetries, all lying close in energy. However, for triplet $\text{Cr}_2(\text{CO})_{10}$, structures were found of six different symmetries, all lying about 10 kcal mol⁻¹ above the singlet structures in energy. Thus the singlet C_{2h} structure is the global energy minimum among all of the $\text{Cr}_2(\text{CO})_{10}$ structures studied. The relative energies of the triplet $\text{Cr}_2(\text{CO})_{10}$ structures and their imaginary harmonic vibrational frequencies are listed in Table 2. For triplet $\text{Cr}_2(\text{CO})_{10}$ (Fig. 2) the fully optimized structures are shown in Figs. 6–11.

Fig. 6 shows the unbridged staggered C_2 structure of the lowest energy B3LYP triplet electronic state, 3B , which is a genuine minimum with both the B3LYP and BP86 methods. However, using the BP86 functional the doubly bridged C_{2h} structure shown in Fig. 7 lies lower than the C_2 structure by 0.1 kcal mol⁻¹. Remarkably, the C_2 and the C_{2h} structures differ considerably in geometry. Furthermore, the C_2 triplet $\text{Cr}_2(\text{CO})_{10}$ is higher in energy than its two constituent singlet fragments of $\text{Cr}(\text{CO})_5$ by 4.1 kcal mol⁻¹ with B3LYP and lower by 3.4 kcal mol⁻¹ with BP86. In order to explore the accommodation of electrons around Cr in terms of the 18-electron rule, the Cr–Cr distance, the Cr–C distances, and the Cr–Cr–C angles in this triplet $\text{Cr}_2(\text{CO})_{10}$ isomer are compared with those in $\text{Cr}_2(\text{CO})_{10}^{2-}$, which is a saturated compound where the Cr–Cr single bond gives each chromium atom the favored 18-electron noble gas configuration. The Cr–Cr distance in $\text{Cr}_2(\text{CO})_{10}$ is computed to be 2.805 Å (B3LYP) and 2.726 Å (BP86), which is significantly shorter than the theoretical Cr–Cr distance of 3.30 Å in the $\text{Cr}_2(\text{CO})_{10}^{2-}$ dianion. This might suggest the existence of a weak Cr=Cr double bond, similar to the oxygen–oxygen double bond in O_2 in which a single Cr–Cr σ bond is complemented by “half bonds” involving a single bonding electron in each of the two perpendicular π orbitals. An organometallic example of a similar triplet metal–metal double bond is the Fe=Fe double bond in $(\eta^5\text{-Me}_5\text{C}_5)_2\text{Fe}_2(\mu\text{-CO})_3$ (**I**), which has been characterized structurally (Fe=Fe of 2.27 Å) and which has been determined experimentally by magnetic measurements to have a magnetic moment of $2.5 \pm 0.1 \mu_B$, corresponding to a triplet ground state.²⁹



I

The Cr–C bond lengths of the five nonequivalent carbonyls in the triplet C_2 symmetry $\text{Cr}_2(\text{CO})_{10}$ are in the range: 1.903 Å–1.946 Å (B3LYP) or 1.873 Å–1.925 Å (BP86). The two methods both show that the axial Cr–C bond lengths are shorter than those of the Cr–C (1.923 Å B3LYP and 1.905 Å BP86) in the constituent $\text{Cr}(\text{CO})_5$ fragments or in $\text{Cr}(\text{CO})_6$ with the experimentally known 1.916 ± 0.002 Å ($r_{\text{Cr-C}}$). This suggests an increased interaction between the chromium and the carbon atoms (along the C_4 axis in the $\text{Cr}(\text{CO})_5$ fragment) leading to formation of the Cr=Cr bond. The corresponding C–O distances remain nearly the same compared to the C–O bond length in the $\text{Cr}(\text{CO})_5$ fragment. In similar fashion to the singlet, the terminal Cr–C–O bond angle closes up from 180° to 172.5° with B3LYP and to 166.5° with BP86. However, these two corresponding carbonyls are no longer in the same plane and have very long distances (2.892 Å B3LYP and 2.628 Å BP86) to the opposite chromium atom. These distances are even longer than the Cr–C long-bridging distance (2.589 Å B3LYP and 2.463 Å BP86) in the singlet C_{2h} minimum. Also, the Cr–Cr–C angles (with the axial carbonyls) are 159.4° (B3LYP) and 150.8° (BP86). This implies a much weaker interaction between the bridging Cr–C in the triplet C_2 structure, providing further indication of greater bond strength than in the three previously discussed singlet structures. Finally, both the Cr–C–O and the C–Cr–C angles remain nearly unchanged compared to the corresponding angles in the $\text{Cr}(\text{CO})_5$ fragments.

Lying close in energy to the C_2 structure but with two bridging carbonyls is the 3B_g electronic state of C_{2h} symmetry shown in Fig. 7. With the BP86 functional it lies the lowest energetically (by about 0.1 kcal mol⁻¹) among the six triplet structures and has all real harmonic vibrational

Table 2 Energies and stationary point characteristics of triplet $\text{Cr}_2(\text{CO})_{10}$. Relative energies refer to the C_{2h} symmetry 1A_g ground state of $\text{Cr}_2(\text{CO})_{10}$

Sym.	State	Figure	Imaginary harmonic vibrational frequencies		Total energy E_h		Relative energy/kcal mol $^{-1}$	
			B3LYP	BP86	B3LYP	BP86	B3LYP	BP86
C_2	3B	6	(none)	(none)	-3222.62407	-3223.04695	12.7	13.2
C_{2h}	${}^3B_g, {}^3B_2$	7	18i(a_{1u})	(none)	-3222.62117	-3223.04714	14.6	13.1
C_{2v}	${}^3A_2, {}^3B_2$	8	74i(b_2)	119i(b_1)	-3222.62011	-3223.03799	15.2	18.9
D_{2h}	${}^3B_{3g}$	9	105i(b_{2g}), 80i(b_{3u})	95i(b_{2g})	-3222.61951	-3223.04692	15.6	13.3
D_{4d}	3A_1	10	509i(e_3)	235i(e_3)	-3222.61362	-3223.03652	19.3	19.8
D_{4h}	${}^3A_{2g}$	11	22i(a_{1u})	363i(e_g), 20i(a_{1u})	-3222.60488	-3223.02812	24.8	25.1

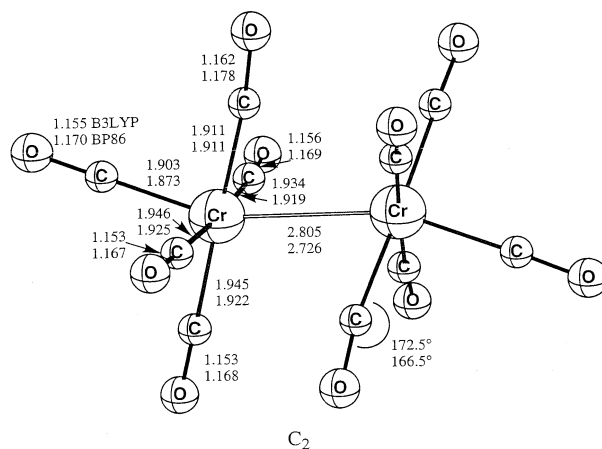


Fig. 6 The unbridged C_2 symmetry B3LYP minimum energy structure for triplet $\text{Cr}_2(\text{CO})_{10}$ predicted from B3LYP and BP86 methods. Distances are reported in Å.

frequencies. However, with the B3LYP functional it has one very small imaginary vibrational frequency of a_{1u} symmetry at 181 cm^{-1} and an energy 2 kcal mol^{-1} higher than the C_2 minimum, indicating that this structure is either a minimum or very close to one. The C_{2h} structures of the singlet and the triplet electronic states differ in three parameters: the Cr–Cr distance, the difference in bridging lengths, and the different Cr–C–O angle. Firstly, the Cr–Cr distance is shortened from 2.928 Å to 2.818 Å (B3LYP) and from 2.832 Å to 2.677 Å (BP86). Secondly, for the longer bridging carbonyl, the B3LYP functional predicts lengthening from 2.589 Å to 2.652 Å whereas BP86 suggests shortening from 2.463 Å to 2.258 Å . Lastly, B3LYP computes the Cr–C–O angle to be 165° , which is nearly the same as in the singlet C_{2h} structure, while BP86 computes the value of 152° , which is much more bent than in the singlet C_{2h} structure, 164° . This not only provides evidence that a double bond for the triplet structure may exist with B3LYP, like the triplet C_2 structure, but also that bridging π interactions may occur similar to those in the singlet C_{2h} structure for BP86.

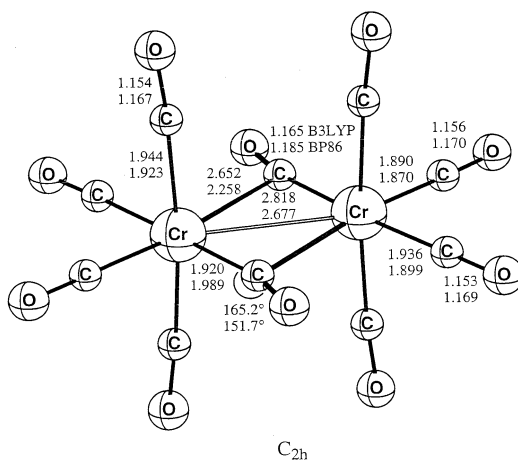


Fig. 7 The dibridged BP86 minimum energy structure for triplet $\text{Cr}_2(\text{CO})_{10}$ with C_{2h} symmetry. This structure has one small imaginary harmonic vibrational frequency for B3LYP and is a genuine minimum with the BP86 method. Distances are reported in Å.

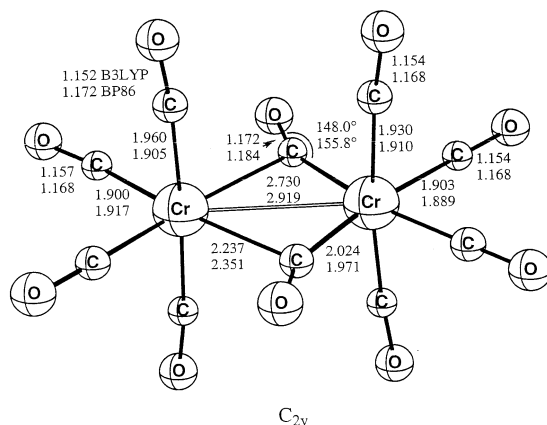


Fig. 8 The dibridged structure for triplet $Cr_2(CO)_{10}$ with C_{2v} symmetry and one imaginary harmonic vibrational frequency with both the B3LYP and BP86 methods. Distances are reported in Å.

The further geometric constraint of forcing the bridging carbonyls to be symmetric leads to the C_{2v} dibridged structure (the 3A_2 electronic state lies lower with B3LYP, and the 3B_2 electronic state lies lower with BP86) shown in Fig. 8. This structure is higher lying energetically by 2.5 kcal mol⁻¹ and 5.7 kcal mol⁻¹ above the triplet minima, namely the C_2 structure, with B3LYP and the C_{2h} structure, with BP86, respectively. The C_{2v} structure has only one imaginary vibrational frequency at 74i cm⁻¹ (b_2 symmetry, B3LYP) and at 119i cm⁻¹ (b_1 symmetry, BP86). This imaginary vibrational frequency shows that the structure is not a minima, since it leads back to the staggered C_2 minimum. Similarly, for BP86, the frequencies lead back to the eclipsed C_{2h} minimum.

Imposing further symmetry constraints on the triplet structure leads to the dibridged D_{2h} structure (${}^3B_{3g}$ electronic state) which is shown in Fig. 9. Similar to the singlet D_{2h} structure (Fig. 5), the dibridged $Cr_2(CO)_{10}$ has the shortest Cr–Cr distance (2.679 Å B3LYP and 2.648 Å BP86) among the nine structures considered here. The bridging Cr–C distances (2.110 Å B3LYP and 2.098 Å BP86) for this structure are longer than the Cr–C bond distance in $Cr(CO)_5$ (1.923 Å B3LYP and 1.905 Å BP86). Thus we assign to this structure a four-center six π electron bond. For the B3LYP method the dibridged D_{2h} $Cr_2(CO)_{10}$ has two imaginary vibrational frequencies: one at 105i cm⁻¹ (b_{2g} symmetry) that corresponds to the C_{2h} structure and one at 80i cm⁻¹ (b_{3u} symmetry)

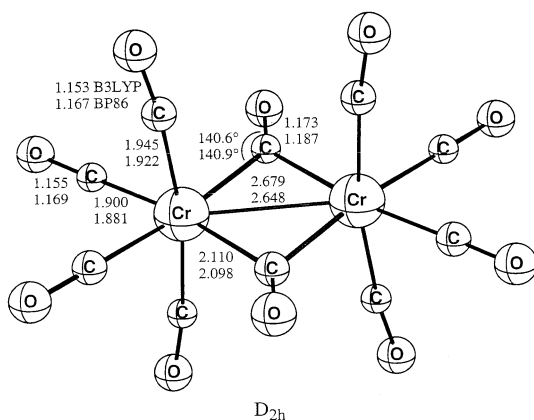


Fig. 9 The dibridged structure for triplet $Cr_2(CO)_{10}$ with D_{2h} symmetry. This structure has two imaginary harmonic vibrational frequencies for B3LYP and one imaginary harmonic vibrational frequency with the BP86 method. Distances are reported in Å.

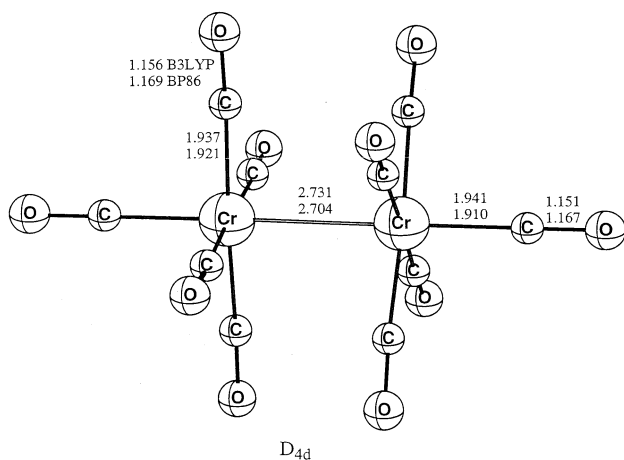


Fig. 10 The staggered nonbridging structure for triplet $\text{Cr}_2(\text{CO})_{10}$ with D_{4d} symmetry. This conformer has one small imaginary harmonic vibrational frequency with B3LYP and two large imaginary harmonic vibrational frequencies with BP86 method. Distances are reported in Å.

that corresponds to the C_{2v} structure. The one imaginary frequency of the BP86 functional, namely a b_{2g} mode, is predicted at $95i \text{ cm}^{-1}$. The energy is $2.9 \text{ kcal mol}^{-1}$ above the triplet minimum C_2 with B3LYP and $0.2 \text{ kcal mol}^{-1}$ above the triplet minimum C_{2h} with BP86. Therefore we conclude that the D_{2h} structure is not a genuine minimum, but energetically very close to the C_{2h} minimum.

Our highest symmetry structures that might formally possess a $\text{Cr}=\text{Cr}$ double bond are the unbridged D_{4d} (3A_1 electronic state) and D_{4h} (${}^3A_{2g}$ electronic state) structures of $\text{Cr}_2(\text{CO})_{10}$ shown in Figs. 10 and 11. Unexpectedly, both the D_{4d} and D_{4h} structures have quite long chromium–chromium distances, for the former 2.731 Å (B3LYP) and 2.704 Å (BP86), and 2.827 Å (B3LYP) or 2.795 Å (BP86) for the latter. The staggered D_{4d} structure (Fig. 10) is qualitatively similar to the eclipsed D_{4h} structure (Fig. 11). However, the latter has a chromium–chromium distance, that is longer by 0.096 Å (B3LYP) and 0.091 Å (BP86), consistent with simple steric repulsion arguments. For the D_{4d} structure the two equatorial and one axial $\text{Cr}-\text{C}$ bond distances are predicted to be 1.937 Å and 1.941 Å (B3LYP), respectively or 1.921 Å and 1.910 Å (BP86), which are quite similar

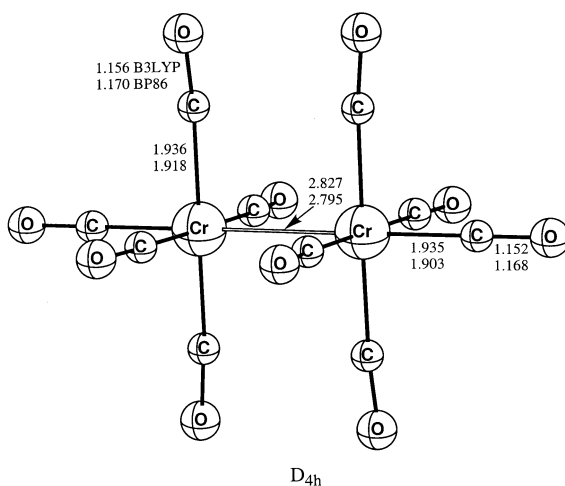


Fig. 11 The eclipsed nonbridging structure for triplet $\text{Cr}_2(\text{CO})_{10}$ with D_{4h} symmetry and one large imaginary harmonic vibrational frequency with both the B3LYP and BP86 methods. Distances are reported in Å.

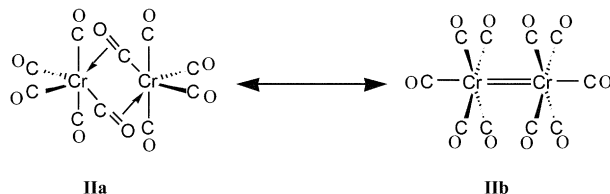
to the corresponding bond lengths of $\text{Cr}(\text{CO})_5$ and to the experimental $\text{Cr}(\text{CO})_6$ distance of 1.916 Å. The axial C–O distances are interesting in that these are identical to the B3LYP and BP86 results for $\text{Cr}(\text{CO})_5$ and the experimental result for $\text{Cr}(\text{CO})_6$. However, the Cr–C distances are slightly longer. This lengthening suggests a very weak interaction between the two equivalent $\text{Cr}(\text{CO})_5$ fragments.

From vibrational frequency analyses neither the D_{4d} nor D_{4h} structure is a true minimum on the potential energy surface. For the D_{4d} structure, both methods yield a degenerate harmonic vibrational frequency, e_3 , at $509i \text{ cm}^{-1}$ (B3LYP) and $235i \text{ cm}^{-1}$ (BP86). For the D_{4h} structure B3LYP yields one harmonic imaginary vibrational frequency of $22i \text{ cm}^{-1}$ (a_{1u}), while BP86 yields three harmonic imaginary vibrational frequencies of $363i \text{ cm}^{-1}$ (e_g) and $20i \text{ cm}^{-1}$ (a_{1u}). The a_{1u} mode (for both B3LYP and BP86) corresponds to an internal rotation changing the symmetry to D_{4d} . Similarly, the BP86 e_g symmetry normal modes lead to the lower symmetry C_{2h} structure.

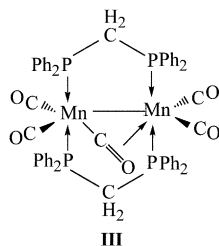
With B3LYP, we have pursued the possibility that the small imaginary vibrational frequency ($22i \text{ cm}^{-1}$, a_{1u}) is fictitious for the D_{4h} structure. As discussed in the Theoretical Methods section, these results are obtained with the (75 302) grid. For the D_{4h} structure of Fig. 11, we reoptimized the B3LYP geometry with the (99 590) numerical integration grid. The B3LYP structure is essentially unchanged, with the Cr–Cr distance decreasing insignificantly from 2.827 Å to 2.826 Å. With the tighter grid the a_{1u} vibrational frequency increases slightly to $24i \text{ cm}^{-1}$. Therefore, we conclude that this imaginary a_{1u} vibrational frequency is genuine and that this structure is extremely close to a structure of slightly lower symmetry.

4. Discussion

The optimized structures for $\text{Cr}_2(\text{CO})_{10}$ may be related to resonance between (a) structure **IIa** with no direct Cr···Cr bond and two special bridging carbonyls donating four electrons each; and (b) structure **IIb** with a Cr=Cr double bond and only terminal CO groups donating two electrons each.

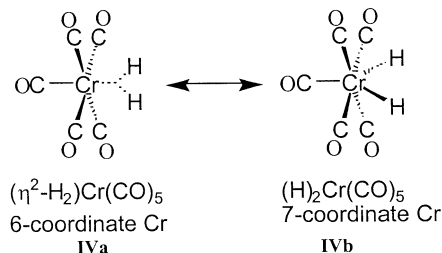


In structure **IIa**, which is favored for singlet $\text{Cr}_2(\text{CO})_{10}$ (Fig. 3), each of the bridging CO groups thus donates a lone pair to one chromium atom through a Cr–C two-electron two-center bond. The latter is similar to the usual bonds between metal atoms and terminal CO groups in most metal carbonyls including $\text{Cr}(\text{CO})_6$. In addition these bridging CO groups donate a second electron pair to the other chromium atom through a longer π -bond from the multiple carbon–oxygen bond. These two bridging carbonyl groups in structure **IIa** are thus similar to the unique bridging carbonyl group in the binuclear manganese carbonyl complex $(\text{Ph}_2\text{PCH}_2\text{PPh}_2)_2\text{-Mn}_2(\text{CO})_4(\mu\text{-CO})$ (**III**), which has been isolated³⁰ and its structure



determined by X-ray diffraction.³¹ Each chromium atom in structure **IIa** for $\text{Cr}_2(\text{CO})_{10}$ uses octahedral sp^3d^2 hybridization to form six bonds to carbonyl groups, sufficient to give each chromium atom the favored 18-electron rare gas configuration, since the two bridging CO groups

each form bonds with such a hybrid from each chromium atom. The pervasive tendency of zero-valent chromium to form such octahedral hybrid orbitals is reflected first in the high stability of octahedral $\text{Cr}(\text{CO})_6$. However, this tendency is also seen in the preference of $\text{H}_2\text{Cr}(\text{CO})_5$, which has been characterized spectroscopically at low temperatures,³² for the structure of a dihydrogen complex $(\text{H}_2)\text{Cr}(\text{CO})_5$ (**IVa**). The latter uses six octahedral hybrid orbitals rather than the dihydride $(\text{H})_2\text{Cr}(\text{CO})_5$ (**IVb**), which requires a less favorable set of seven hybrid orbitals, presumably some type of sp^3d^3 hybrid.



The lowest energy structure for triplet $\text{Cr}_2(\text{CO})_{10}$ (Fig. 6) is a $\text{Cr}=\text{Cr}$ doubly bonded structure (**IIb**) having only terminal CO groups. In this structure the $\text{Cr}=\text{Cr}$ double bond consists of two perpendicular one-electron π “half-bonds” (designated $2/2 \pi$ here and in our abstract) similar to the $\text{O}=\text{O}$ bond in O_2 or the $\text{Fe}=\text{Fe}$ bond in $(\eta^5\text{-Me}_5\text{C}_5)_2\text{Fe}_2(\mu\text{-CO})_3$ (**I**). Assuming that the metal–metal bond axis is the z -axis, these perpendicular one-electron π -half-bonds use the metal d_{xz} and d_{yz} orbitals, which are not involved in the $\text{sp}^3\text{d}^2(z^2, x^2 - y^2)$ octahedral hybridization of each chromium atom required for the six σ bonds (*i.e.*, the bonds to the five terminal CO groups and the $\text{Cr}-\text{Cr}$ σ -bond). In the symmetry point group for the lowest energy triplet $\text{Cr}_2(\text{CO})_{10}$ structure (C_2), the metal d_{xz} and d_{yz} orbitals are not strictly degenerate since the C_2 point group has only non-degenerate irreducible representations. This differs from both the $D_{\infty h}$ point group of O_2 and the D_{3h} local symmetry of the $\text{Fe}=\text{Fe}$ bond in $(\eta^5\text{-Me}_5\text{C}_5)_2\text{Fe}_2(\mu\text{-CO})_3$ (**I**) in which the metal d_{xz} and d_{yz} orbitals belong to the two-fold degenerate irreducible representations e'' and π_g , respectively. However, the analysis of the imaginary vibrational frequencies for D_{4h} triplet $\text{Cr}_2(\text{CO})_{10}$ discussed above suggests that the lowest energy C_2 structure for triplet $\text{Cr}_2(\text{CO})_{10}$ (Fig. 6) may be very close to the D_{4h} structure (Fig. 11), differing only by tilting the $\text{Cr}(\text{CO})_5$ “halves” of local C_4 symmetry. If this is the case, then the energy difference between the metal d_{xz} and d_{yz} orbitals in the C_2 structure of triplet $\text{Cr}_2(\text{CO})_{10}$ may be smaller than the pairing energy of the two electrons so that a triplet rather than a singlet structure is preferred. Note that in the D_{4h} point group the metal d_{xz} and d_{yz} orbitals belong to the two-fold degenerate irreducible representation E_g .

Acknowledgements

We are grateful for the support of this work by NSF Grant CHE-0136186. We also thank Joseph Kenny for helpful discussions and technical assistance with the computations.

References

- 1 I. S. Ignatyev, H. F. Schaefer, R. B. King and S. T. Brown, *J. Am. Chem. Soc.*, 2000, **122**, 1989.
- 2 Y. Xie, H. F. Schaefer and R. B. King, *J. Am. Chem. Soc.*, 2000, **122**, 8746.
- 3 J. P. Kenny, R. B. King and H. F. Schaefer, *Inorg. Chem.*, 2001, **40**, 900.
- 4 W. Kohn and L. J. Sham, *Phys. Rev. A*, 1965, **140**, 1133.
- 5 I. T. Horvath, G. Bor, M. Garland and P. Pino, *Organometallics*, 1986, **5**, 1441.
- 6 M. L. Green, *J. Organomet. Chem.*, 1995, **500**, 127.
- 7 N. A. Richardson, Y. Xie, R. B. King and H. F. Schaefer, *J. Phys. Chem. A*, 2001, **105**, 11 134.
- 8 L. A. Barnes, B. W. Liu and R. Lindh, *J. Chem. Phys.*, 1993, **98**, 3978.
- 9 B. Rees and A. Mitschler, *J. Am. Chem. Soc.*, 1976, **98**, 7918.
- 10 E. Hey-Hawkins and H. G. von Schnering, *Chem. Ber.*, 1991, **124**, 1167.
- 11 I. Lee, S. J. Geib and N. H. Copper, *Acta Crystallogr., Sect. C*, 1996, **C52**, 292.
- 12 H. Borrmann, A. M. Pirani and G. J. Schrobilgen, *Acta Crystallogr., Sect. C*, 1997, **C53**, 19.
- 13 J. R. Phillips and W. C. Trogler, *J. Phys. Chem.*, 1992, **198**, 633.

- 14 T. R. Fletcher and R. N. Rosenfeld, *J. Am. Chem. Soc.*, 1985, **107**, 2203.
- 15 T. Dunning, *J. Chem. Phys.*, 1970, **53**, 2823.
- 16 S. Huzinaga, *J. Chem. Phys.*, 1965, **42**, 1293.
- 17 A. J. H. Wachters, *J. Chem. Phys.*, 1970, **52**, 1033.
- 18 D. M. Hood, R. M. Pitzer and H. F. Schaefer, *J. Chem. Phys.*, 1979, **71**, 705.
- 19 T. Ziegler, *Can. J. Chem.*, 1995, **73**, 743.
- 20 A. D. Becke, *J. Chem. Phys.*, 1993, **98**, 5648.
- 21 C. Lee, W. Yang and R. G. Parr, *Phys. Rev. B*, 1988, **37**, 785.
- 22 A. D. Becke, *Phys. Rev. A*, 1988, **38**, 3098.
- 23 J. P. Perdew, *Phys. Rev. B*, 1986, **33**, 8842; J. P. Perdew, *Phys. Rev. B*, 1986, **34**, 7046.
- 24 V. Jonas and W. Thiel, *Organometallics*, 1998, **17**, 353.
- 25 Gaussian 94 (Revision B. 3), M. J. Frisch, G. W. Trucks, H. B. Schlegel, P. M. W. Gill, B. G. Johnson, M. A. Robb, J. R. Cheeseman, T. Keith, G. A. Petersson, J. A. Montgomery, K. Raghavachari, M. A. Al-Laham, V. G. Zakrzewski, J. V. Ortiz, J. B. Foresman, J. Cioslowski, B. B. Stefanov, A. Nanayakkara, M. Challacombe, C. Y. Peng, P. Y. Ayala, W. Chen, M. W. Wong, J. L. Andres, E. S. Replogle, R. Gomperts, R. L. Martin, D. J. Fox, J. S. Binkley, D. J. Defrees, J. Baker, J. P. Stewart, M. Head-Gordon, C. Gonzalez and J. A. Pople, Gaussian, Inc., Pittsburgh PA, 1995.
- 26 E. Hey-Hawkins and H. G. von Schnering, *Chem. Ber.*, 1991, **124**, 1167.
- 27 I. Lee and N. H. Cooper, *Acta Crystallogr., Sect. C*, 1996, **C52**, 292.
- 28 A. Jost, B. Rees and W. B. Yelon, *Acta Crystallogr., Sect. B*, 1975, **B31**, 2649.
- 29 J. P. Blaha, B. E. Bursten, J. C. Dewan, R. B. Frankel, C. L. Randolph, B. A. Wilson and M. S. Wrighton, *J. Am. Chem. Soc.*, 1985, **107**, 4561.
- 30 R. Colton and C. J. Commons, *Aust. J. Chem.*, 1975, **28**, 1673.
- 31 C. J. Commons and B. F. Hoskins, *Aust. J. Chem.*, 1975, **28**, 1663.
- 32 R. K. Upmacis, M. Poliakoff and J. J. Turner, *J. Am. Chem. Soc.*, 1986, **108**, 3645.